Journal of Experimental Botany, Vol. 63, No. 15, pp. 5545–5558, 2012
doi:10.1093/jxb/ers209 Advance Access publication 21 August, 2012
This paper is available online free of all access charges (see http://jxb.oxfordjournals.org/open_access.html for further details)

Journal of Experimental Botany
www.jxb.oxfordjournals.org

RESEARCH PAPER

The R2R3 MYB transcription factors FOUR LIPS and MYB88 regulate female reproductive development

Srilakshmi Makkena[1,2], Eunkyoung Lee[3], Fred D. Sack[3] and Rebecca S. Lamb[2],*

[1] Plant Cellular and Molecular Biology Graduate Program, The Ohio State University, Columbus, OH 43210, USA
[2] Department of Molecular Genetics, The Ohio State University, Columbus, OH 43210, USA
[3] Department of Botany, The University of British Columbia, Vancouver, BC, Canada V6T 1Z4

*To whom correspondence should be addressed. E-mail: lamb.129@osu.edu

Received 9 March 2012; revised 21 June 2012; accepted 25 June 2012

Abstract

Gamete formation is an important step in the life cycle of sexually reproducing organisms. In flowering plants, haploid spores are formed after the meiotic division of spore mother cells. These spores develop into male and female gametophytes containing gametes after undergoing mitotic divisions. In the female, the megaspore mother cell undergoes meiosis forming four megaspores, of which one is functional and three degenerate. The megaspore then undergoes three mitotic cycles thus generating an embryo sac with eight nuclei. The embryo sac undergoes cellularization to form the mature seven-celled female gametophyte. Entry into and progression through meiosis is essential for megasporogenesis and subsequent megagametogenesis, but control of this process is not well understood. *FOUR LIPS* (*FLP*) and its paralogue *MYB88*, encoding R2R3 MYB transcription factors, have been extensively studied for their role in limiting the terminal division in stomatal development by direct regulation of the expression of cell cycle genes. Here it is demonstrated that *FLP* and *MYB88* also regulate female reproduction. Both *FLP* and *MYB88* are expressed during ovule development and their loss significantly increases the number of ovules produced by the placenta. Despite the presence of excess ovules, single and double mutants exhibit reduced seed set due to reduced female fertility. The sterility results at least in part from defective meiotic entry and progression. Therefore, *FLP* and *MYB88* are important regulators of entry into megasporogenesis, and probably act via the regulation of cell cycle genes.

Key words: *Arabidopsis thaliana*, female sterility, FLP, gametogenesis, MYB88, plant reproduction, transcription

Introduction

Plants are characterized by the alternation of haploid (gametophyte) and diploid (sporophyte) generations. In angiosperms, such as *Arabidopsis thaliana*, the gametophyte is short lived and develops within the sporophytic tissue of the flower. The female gametophyte, or embryo sac, develops within ovules contained in the ovary of the pistil. Ovule primordia develop from placental tissue in the ovary. Along the proximal–distal axis an ovule primordium consists of three distinct regions: the funiculus, the chalaza, and the nucellus. Within the nucellus the megaspore mother cell (MMC) is formed, which divides first meiotically and then mitotically to form the embryo sac (reviewed in Berger and Twell, 2011). The MMC divides meiotically to make four haploid megaspores, of which three degenerate and one, the proximal chalazal megaspore, continues to develop. This functional megaspore increases in size and undergoes a series of nuclear divisions to form an eight-nuclei embryo sac. Then cellularization takes place, dividing the embryo sac into seven cells with four cell types: three antipodal cells at the chalazal end, a diploid central cell, and two synergids and the egg cell at the micropylar end. Antipodal cells, which have no currently known function,

degenerate before fertilization in *Arabidopsis*. The central cell, the egg cell, and the synergid cells form the female germ unit.

Proper specification of the MMC, entry into and completion of meiosis, control of mitotic divisions, and cell fate determination and differentiation are essential for development of the embryo sac. In *Arabidopsis*, a number of genes are known to regulate these processes. For example, mutations in a gene encoding a type I MADS-box transcription factor, *AGL23*, block the first nuclear division of the functional megaspore (Colombo *et al*., 2008). Mutations in the *PROLIFERA* (*PRL*) gene, encoding the DNA replication licensing factor subunit MCM7, arrest the embryo sac with one nucleus (Springer *et al*., 2000). Temporal and spatial regulation of cellularization of the syncytial embryo sac is critical for gametophytic development and cell fate. In the female sterile mutant *hadad* (*hdd*), the gametophyte becomes prematurely cellularized after the first or second gametophytic division (Moore *et al*., 1997). Simultaneously with cellularization, cell fate within the embryo sac is acquired and differentiation begins. *MYB98* encodes an R2R3-MYB transcription factor specifically expressed in the synergid cells. *myb98* mutants fail to form the filiform apparatus and are unable to guide the pollen tube to the micropyle (Punwani *et al*., 2007). However, although many genes are known that are involved in meiotic recombination and other aspects of the meiotic cycle (reviewed in Ma, 2006), how MMC entry into meiosis is controlled is still not known.

The atypical R2R3-MYB transcription factor FOUR LIPS (FLP) and its paralogue MYB88 have been well characterized for their partially redundant roles in stomatal patterning. *FLP* was first identified during a mutant screen (Yang and Sack, 1995), while *MYB88* was identified by sequence similarity with *FLP* (Lai *et al*., 2005). These genes have overlapping functions in restricting the last precursor cell in the stomatal lineage, the guard mother cell (GMC), to a single symmetric division and also promoting guard cell differentiation. In loss-of-function *flp-1* and *flp-7* alleles, the GMC undergoes extra divisions resulting in clusters of four or more guard cells in contact with one another. *flp-1; myb88* double mutants exhibit more severe stomatal phenotypes than the single *flp-1* mutation alone, while single *myb88* mutants show no discernible defects in stomata. In addition, the cells in stomatal clusters do not properly differentiate into guard cells. Thus, *FLP/MYB88* are required both for limiting the GMC to a single symmetric division and for the subsequent differentiation of guard cells (Lai *et al*., 2005).

As DNA-binding transcription factors, FLP and MYB88 directly regulate the expression of a number of genes, including cell cycle genes (Xie *et al*., 2010a; Vanneste *et al*., 2011). FLP has been shown to bind to the promoter of *CDKB1;1*, a mitosis-inducing factor, and to reduce its expression. *CDKB1;1* along with the closely related gene *CDKB1;2* is required both for the last division in the stomatal pathway (Boudolf *et al*., 2004) and for the overproliferation of guard cells in *flp* mutants (Xie *et al*., 2010a). It has been proposed that *FLP* and *MYB88* together regulate stomatal patterning by controlling cell cycle progression and terminal differentiation through multiple cell cycle targets (Xie *et al*., 2010a). In addition to *CDKB1;1*, FLP/MYB88 are also necessary to repress expression in a timely manner of the plant A2-type cyclin-encoding gene *CYCA2;3* in newly formed guard cells to promote exit from the cell cycle (Vanneste *et al*., 2011).

Although their function in epidermal patterning is best described, *FLP* and *MYB88* are also required for abiotic stress tolerance since *flp-1*; *myb88* double mutants have reduced expression of stress-induced genes and are more susceptible to both drought and salt stress (Xie *et al*., 2010b). FLP/MYB88 positively and directly regulate the expression of at least some stress-responsive genes, suggesting that changes in the stress transcriptome in *flp-1; myb88* mutants are not just an indirect effect of abnormal stomatal complexes. For example, FLP/MYB88 positively regulate the *NAC019* gene, involved in response to dehydration, abscisic acid (ABA), and salt (Tran *et al*., 2004), by binding directly to its promoter (Xie *et al*., 2010b). *FLP* and *MYB88* are likely to have other developmental functions as well since they are expressed in a wide variety of tissues. *FLP* is expressed in developing stomata, specifically in GMCs just before their symmetric division. Expression is also seen in organs without stomata, including the root (Lai *et al*., 2005). However, whether *FLP* and *MYB88* have any developmental roles other than stomatal development has not been investigated.

Here, genetic and cell-biological evidence is provided that *FLP* and *MYB88* function during female reproductive development in *Arabidopsis*. In loss-of-function *flp* single and *flp; myb88* double mutants, the placenta produces extra ovule primordia, suggesting these genes normally restrict the proliferation of this tissue. However, seed set is reduced. The reduction is the result of defects in female megasporogenesis. The expressivity of the defect is influenced by genetic background. In a subset of mutant ovules the MMC either fails to divide meiotically or divides abnormally, leading to a lack of female gametophyte development. In contrast to the embryo sac defects, mutant pollen developed and functioned normally. Therefore, FLP and MYB88 function as positive transcriptional regulators of entry into megasporogenesis.

Materials and methods

Plant material and growth conditions

The following alleles of *FLP* were used in this study: *flp-1*, *flp-7*, *flp-8*, and *SALK_033970*. In addition, two double mutants were also analysed: *flp-1; myb88* and *flp-7; myb88*. *flp-7* and *flp-8* are in the Landsberg *erecta* (L. *er*) background whereas *flp-1*, *flp-1*; *myb88*, *SALK_033970*, and *flp-7; myb88* are all in the Columbia-0 (Col-0) background as previously reported (Lai *et al*., 2005). Genotyping was performed as described, using primer combinations listed in Supplementary Table S1 available at *JXB* online (primer sequences are given in Supplementary Table S2). Various female gametophyte-specific marker lines (Supplementary Table S3) were introgressed into the *flp-7* background by crossing homozygous mutant plants to the marker lines and allowing the F_1 to self-fertilize. PCR genotyping of the segregating F_2 population was performed and the presence of the marker gene was identified by selecting seedlings on Murashige and Skoog (MS) plates containing kanamycin at 50 μg ml^{-1}.

Arabidopsis seeds were cold treated for 3 d at 4 °C and germinated and grown on Fafard 2 mix soil (Fafard) under long-day (16 h, 80 μmol m^{-2} s^{-1}) irradiance either in controlled growth chambers (Enconair Ecological Chambers Inc., Manitoba, Canada) or in growth rooms with subirrigation at 22 °C with 60% relative humidity. Seeds grown on plates were sterilized with 70% ethanol followed by 10% (v/v)

hypochlorite and 0.1% SDS, and placed on Petri dishes containing MS media (RP1 Corp.) with 1% plant agar with or without antibiotic. The plates were incubated in the dark at 4 °C for 5 d to achieve uniform germination and then moved to a CU-36L growth chamber (Percival Scientific Inc., Perry, IA, USA) and grown under long-day conditions (22 °C; 16 h photoperiod) unless noted. Seedlings were transplanted to soil at ~2 weeks old.

PCR-based genotyping

Genomic DNA was extracted as previously described (Teotia and Lamb, 2009). Primer combinations and primer sequences are shown in Supplementary Tables S1 and S2 at *JXB* online, respectively. PCR was done using Biolase Red DNA Polymerase (Bioline) on a conventional PCR machine (Bio-Rad-iCycler Thermal Cycler). *flp-1*, *flp-7*, and *er* alleles were identified by derived cleaved amplified polymorphic sequences (dCAPS; see Supplementary Table S1) (Neff *et al*., 1998, 2002). The *flp-1* allele was genotyped as described (Xie *et al*., 2010a).

Seed set and fertility analysis

In order to analyse the seed set of the mutants and wild type, plants were grown under long-day conditions. Seeds of various genotypes were sown in 4 inch round pots. Four plants per genotype were used for comparing the percentage seed set. The total number of ovules and the number of seeds present in the first 15 siliques on the primary inflorescence only were counted, as previously described (Alvarez and Smyth, 1999). The percentage seed set was calculated by taking into account the total number of ovules and the number of seeds present in a silique. Statistical significance of the values was calculated using a Student's *t*-test.

Reciprocal crosses were done to test male and female fertility by emasculating and hand pollinating 15 flowers of each genotype, as previously described (Unte *et al*., 2003). The number of seeds made in each silique was counted after the siliques were fully matured. Statistical significance of the values was calculated as above.

Aniline blue staining of pollen tubes and mucilage staining of seeds

Aniline blue staining of pistils was done according to Jiang *et al*. (2005). Flowers were emasculated just prior to pollination (late stage 12) and were grown for another 18–24 h to allow transmitting tract and ovule development to finish. Pistils were hand pollinated and grown for a further 24 h to allow pollen tube growth. Pollinated pistils were fixed in a solution of ethanol:acetic acid (3:1) for 2 h at room temperature, washed three times with ddH_2O, softened in 8 M NaOH overnight, and washed in ddH_2O several times before staining. Pistils were stained in aniline blue solution (0.1% aniline blue in 0.1 M K_2HPO_4–KOH buffer, pH 11) for 3 h in the dark. The stained pistils were observed and photographed with a Nikon Eclipse 80i fluorescence microscope.

Mucilage production by *flp-7* and *flp-1; myb88* seeds was analysed according to Debeaujon *et al*. (2000). In brief, seeds were soaked in 0.03% ruthenium red (w/v) for 15 min and washed in water before being mounted on a slide and observed using a Nikon Digital Sight DS-5M camera on a Nikon SMZ800 dissecting microscope.

Ovule clearing and differential interference contrast (DIC) optics

Definitions for floral, ovule, and gametophyte development stages were as described in Smyth *et al*. (1990), Christensen *et al*. (1997), and Schneitz *et al*. (1995). Embryo sacs were collected from the entirety of the primary inflorescence and also secondary inflorescences. To examine mature ovules, flowers were emasculated just prior to pollination (late stage 12) and were grown for another 24 h. Ovule clearing and microscopy was done according to Rodrigo-Peiris *et al*. (2011), with some modifications. Pistils were opened along the carpel margins and fixed in a solution of 9:1 absolute ethanol:glacial acetic acid overnight at 4 °C followed by washing in 90% ethanol for 1 h, and stored in 70% ethanol until examination. Ovules were cleared in chloral hydrate (8 g of chloral hydrate and 2 ml of ddH_2O to each ml of glycerol) on microscope slides for 2 h before microscopic analysis with DIC optics on a Nikon Eclipse 90i Microscope. Pictures were taken using the attached Nikon camera and analysed with NIS elements Advanced Research software version 3.0.

β-Glucuronidase (GUS) staining

Histochemical staining for GUS activity was performed as described (Jefferson *et al*., 1987). In brief, ovules were collected from pistils at different stages of flower development. The ovules were incubated in GUS staining buffer (50 mM sodium phosphate buffer pH 7.0, 10 mM EDTA, 2 mM potassium ferricyanide, 2 mM potassium ferrocyanide, 0.1% Triton X-100, and 2 mM 5-bromo-4-chloro-3-indolyl-β-D-glucuronic acid) at 37 °C for 72 h. Ovules were then washed in 90% ethanol for 1 h and stored in 70% ethanol until examination. Photographs were taken using a Nikon Digital Sight DS-5M camera attached to a Nikon Eclipse 80i compound microscope.

Confocal microscopy of ovules

Ovules were collected from pistils at different stages of flower development and were incubated in 0.5% propidium iodide in 50 mM phosphate buffer at room temperature or in 10 μg ml^{-1} of propidium iodide. Ovules were observed using either a Nikon D-Eclipse C1si or Nikon Eclipse 80i confocal microscope at excitation wavelengths of 488 nm and 543 nm. Emission was collected at 620–720 nm and 488–562 nm to visualize propidium iodide and green fluorescence protein (GFP) fluorescence, respectively.

Results

FLP *and* MYB88 *are expressed in the flower*

To characterize *FLP* and *MYB88* expression during reproductive development, transgenic plants containing either a *pFLP::GUS-GFP* construct (Lai *et al*., 2005) or a *pMYB88::GUS-GFP* construct (Vanneste *et al*., 2011; a kind gift of Steffen Vanneste) were used. *FLP* expression was detected in unopened flower buds, at the bases of sepals, petals, and stamens and in the receptacle of carpels (Fig. 1A, 1B, and data not shown). *pFLP::GUS-GFP* is strongly expressed in the placenta within the ovary (Fig. 1C). Additionally, expression of *FLP* can be seen in both the style (Fig. 1D) and stigma (Fig. 1E) of the pistil. During ovule development, *FLP* has a dynamic expression pattern. During early stages of ovule development (before integuments are morphologically distinct), *FLP* expression was barely detectable (Fig. 1F). However, once integument outgrowth has begun, strong *FLP* expression is seen in the funiculus (Fig. 1G), which persists into later stages (Fig. 1H, 1I). Notably, the *FLP* promoter drives expression in the nucellus in younger ovules, where it is specifically expressed in the MMC and in epidermal cells (Fig. 1H). *FLP* is also expressed in the integuments, starting at a low level when they initiate (Fig. 1H). Later in ovule development it is expressed in the endothelial layer (the adaxial layer of the inner integument) and the outer layer of the outer integument, which will form the mucilage-containing seed coat cells (Fig. 1I, 1J). In contrast, little to no expression was seen in older anthers (Fig. 1B), consistent with Genevestigator data (Zimmermann *et al*., 2004, 2005). *MYB88* is expressed at a much lower level than *FLP* (Lai *et al*., 2005). However, *MYB88*

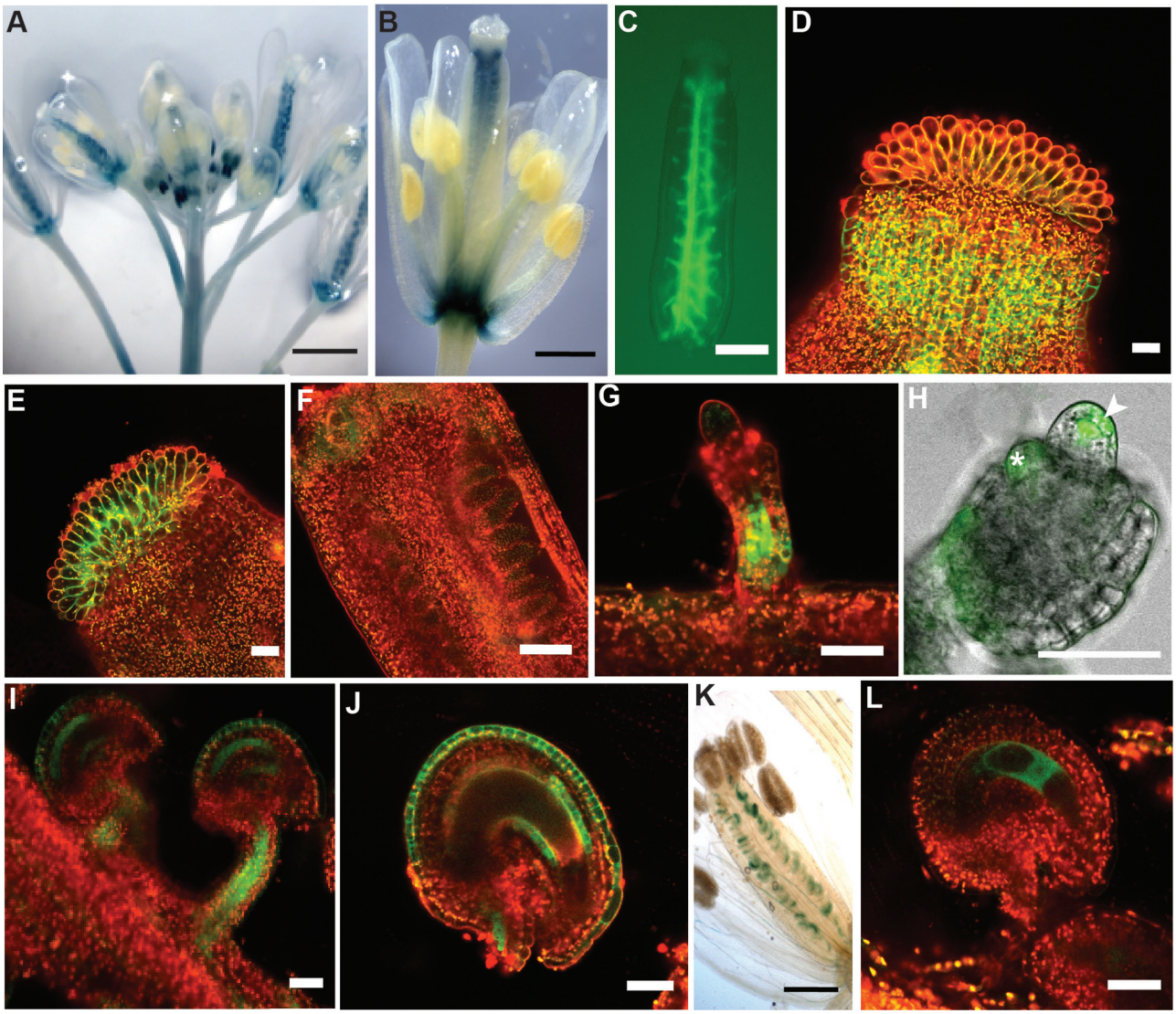

Fig. 1. *FLP* and *MYB88* are expressed in reproductive organs. (A–J) Micrographs of *pFLP::GUS-GFP* transgenic plants. (A and B) GUS staining. (C–J) GFP fluorescence visualized using confocal microscopy. (A) *FLP* expression in whole inflorescence. (B) *FLP* is expressed in the carpel. (C) Expression of *FLP* can be seen in the placenta. (D) *FLP* is expressed in the style. (E) *FLP* is expressed in the stigmatic tissue. (F) During early ovule development, before integument initiation, little *FLP* expression is detectable within the ovule. (G) Expression of *FLP* can be seen in the funiculus as the integuments are initiating. (H) *FLP* is expressed in the nucellus, including epidermal cells (arrowhead) and the MMC. FLP is also expressed in initiating integuments (asterisk) and the funiculus. (I) *FLP* expression persists in the funiculus and is seen in the integuments of older ovules. (J) In stage 13 ovules, *FLP* is expressed in both the endothelial layer and the outer layer of the outer integument. (K and L) Micrographs of *pMYB88::GUS-GFP* transgenic plants. (K) GUS staining showing *MYB88* expression in ovules. (L) In stage 13 ovules, *MYB88* is expressed in the embryo sac.

expression is detected in ovules (Fig. 1K) and in the embryo sac of stage 13 flowers (Fig. 1L).

Loss of FLP *and* MYB88 *reduces female fertility*

To investigate the roles of *FLP* and *MYB88* in reproductive development, fruit size and seed set were examined in different *flp* alleles and double mutants with *myb88*. The siliques of both *flp-7* and *flp-1; myb88* appeared shorter than their respective wild types (Fig. 2A, 2B). Mutant siliques contain small, white ovules that appear to be either aborted or not fertilized (Fig. 2A, 2B, 2D; Table 1), consistent with the presence of shorter siliques. The seed set of *flp* and *myb88* mutants was then compared with that of their respective wild type (L. *er* or Col-0). All examined *flp* and *flp; myb88* plants except *flp-1* have significantly reduced seed set (Table 1). Interestingly, *flp-7*, *flp-8*, *SALK_033970* (which is a loss-of-function allele in the *FLP* locus), and *flp-7; myb88* have significantly more ovules than the wild type, but still have reduced seed set (Table 1). This suggests that the ovary and placenta are larger in pistils of *flp* mutants, but that the reduced fertility leads to smaller fruits. These results show that *FLP* and *MYB88* regulate reproductive development. None of the available *flp* alleles is RNA null, although the *myb88* allele is a knockdown (Lai *et al*., 2005). This makes it difficult to assess

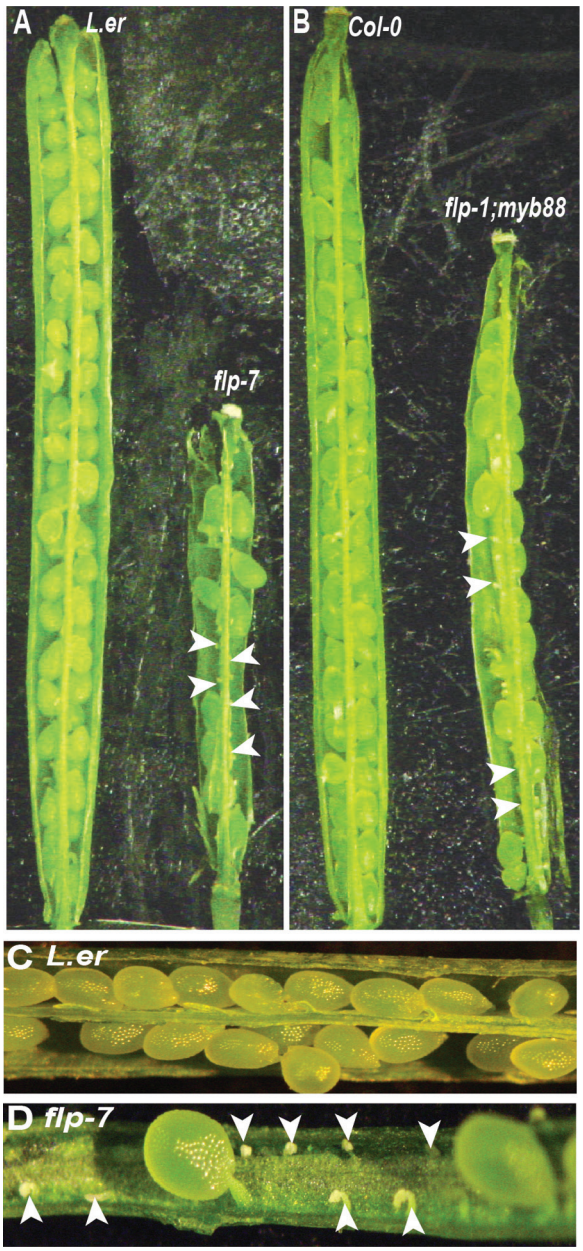

Fig. 2. Fertility is lowered in *flp-7* and *flp-1; myb-88* plants. Dissecting microscope images of siliques. (A) *flp-7* fruit are shorter than those of the wild type and contain aborted ovules (arrowheads). (B) *flp-1; myb88* fruit are shorter than those of the wild type and contain aborted ovules. (C) L. *er* silique containing many seeds. (D) *flp-7* silique containing a few seeds and several aborted ovules (arrowheads).

the extent to which *FLP* function is lost in these backgrounds. For example, both *flp-1* and *flp-7* mutations are in the 3' splice site AG of introns (3 and 4, respectively) and both have been shown to cause splicing errors (Lai *et al*., 2005). These errors are predicted to result in premature translational stops within the MYB domain (in the third R2 helix in *flp-1* and after the first R3 helix in *flp-7*), thus producing truncated proteins likely to have disrupted activity. Despite the fact that these alleles are predicted to produce similar truncation products, the stomatal defects seen in *flp-7* are more severe than those of *flp-1* (Lai *et al*., 2005). As *flp-7* (L. *er*) and *flp-1; myb88* (Col-0) display significantly reduced seed set and are in two different genetic backgrounds, they were selected for further studies.

The strong expression of *FLP* in integuments (Fig. 1I, 1J) suggests that this gene may be involved in development of the seed coat. Mature seeds of *flp-7* and *flp-1; myb88* were compared with their respective wild types. Although some minor variability in seed shape was observed in the mutant seeds (Supplementary Fig. S1 at *JXB* online), particularly *flp-7*, no noticeable germination defects were observed (data not shown). In addition, mucilage was produced by both *flp-7* and *flp-1; myb88* seeds (Supplementary Fig. S1), suggesting that differentiation of the seed coat is not significantly altered.

To determine whether the reduced seed set is due to male and/or female infertility, reciprocal crosses were made using *flp-7* or *flp-1; myb88* homozygous plants and the wild type. Both *flp-7* and *flp-1; myb88* siliques harboured fewer seeds than their respective wild types when pollinated with either wild-type or mutant pollen (Table 2), indicating that female fertility is compromised. *flp-7* pollen, when used to fertilize wild-type pistils, resulted in slightly reduced seed set (Table 2). However, the fertility of *flp-1; myb88* pollen was comparable with that of the wild type. Taken together, these results suggest that *FLP* and *MYB88* function in female reproduction.

Embryo sac development is altered by loss of FLP *and* MYB88

The aborted ovules seen in siliques of *flp* mutants could be caused by defects in ovule and/or embryo sac development or by lack of fertilization. Stigmatic and transmitting tract tissues in the carpel are required for proper pollen tube growth and fertilization. Mutants with reduced growth of these tissues have reduced fertility due to poor pollen tube growth (Heisler *et al*., 2001; Gremski *et al*., 2007). *FLP* is strongly expressed in the stigma and style of the pistil (Fig. 1D, 1E), suggesting that it could function in these tissues. In order to examine whether pollen tube growth is affected in *flp* mutants, carpels were stained with aniline blue 24 h after pollination. In both L. *er* and *flp-7* pistils, pollen tubes grew throughout the transmitting tract and into ovules (Supplementary Fig. S2 at *JXB* online), indicating that the reduced seed set in *flp* alleles is not due to defects in either the stigma or transmitting tract.

Since pollen tubes were able to travel to the ovules, the reduced fertility seen in *flp-7* and *flp-1; myb88* plants is probably due to ovule and/or female gametophyte defects. Therefore, ovules were examined 2 d after emasculating flowers at stage 13 (according to Smyth *et al*., 1990) to determine whether ovule development proceeded normally. The morphology of mutant ovules at female gametophyte developmental stage 7 (FG7; Christensen *et al*., 1997) appeared normal, with fully developed outer and inner integuments and well-differentiated proximal–distal polarity (Fig. 3B, 3D), suggesting that ovule development is intact in these mutants. The FG7 embryo sacs of *flp-7* and *flp-1; myb88* were then compared with their respective wild types, L. *er* and Col-0. Ninety percent of L. *er* ($n = 281$) and 97% of Col-0 ($n = 607$) ovules display four visible

Table 1. flp *and* flp; myb88 *mutants have reduced fertility that is influenced by genetic background*

Genotype	Ovules per silique[a]	Seeds per silique[a]	Aborted ovules per silique[a,b]	Seed set
L. *er*	45 ± 0.6	42 ± 1.0	3 ± 0.6	94%
L. *er/pER::ER*	58 ± 0.8	53 ± 0.7	5 ± 0.3	92%
flp-7	61 ± 0.9**	4 ± 0.7**	57 ± 1.3**	6%
flp-7/pER::ER	54 ± 1.4***	17 ± 0.5****	40 ± 1.3****	31%
flp-8	66 ± 0.8**	46 ± 2.1	20 ± 0.6**	70%
Col-0	48 ± 0.5	39 ± 1.5	9 ± 1.5	80%
flp-1	47 ± 0.7	34 ± 1.7	13 ± 1.6	72%
SALK_033970/flp	54 ± 0.8**	37 ± 3.4	17 ± 2.7*	63%
flp-1; myb88	49 ± 0.7	14 ± 2.4**	35 ± 2.1**	27%
flp-7; myb88	68 ± 0.7**	47 ± 3.1*	21 ± 3.2**	69%

[a] Values are means ±SE (n = 60) or means ±SE of n = 60 for three independent transgenic lines (180 siliques in total) for L. *er/pER::ER* and *flp-7/pER::ER*.
[b] Defined as small white ovules with no evidence of embryo or seed development.
*Values that are significantly different from the wild type at $P < 0.05$. **Values that are significantly different from the wild type at $P < 0.01$.
***Values that are significantly different from L. *er/pER::ER* at $P < 0.05$. ****Values that are significantly different from L. *er/pER::ER* at $P < 0.01$.

Table 2. *Loss of* FLP *and* MYB88 *compromises female fertility*

Female parent	Male parent	Seeds per crossed silique[a]
L. *er*	L. *er*	43.7 ± 6.1**
	flp-7	37.8 ± 25.0*
flp-7	L. *er*	14.6 ± 6.2**
	flp-7	14.9 ± 7.5**
Col-0	Col-0	40.3 ± 4.7
	flp-1; myb88	42.6 ± 6.3
flp-1; myb88	Col-0	7.3 ± 9.4**
	flp-1; myb88	2.1 ± 4.7**

[a] Values are the mean ±SE (n = 15).
*Values that are significantly different from the wild type at $P < 0.05$.
**Values that are significantly different from the wild type at $P < 0.01$.

nuclei, corresponding to the egg cell, central cell, and two synergids (Fig. 3E). Although Polygonum-type embryo sacs, such as those found in *Arabidopsis*, contain seven cells of four types (Yadegari and Drews, 2004), in *Arabidopsis* the three antipodal cells have degenerated by FG7 (Christensen *et al*., 1997). In contrast to the wild type, only 56% of *flp-7* (n=337) and 78% of *flp-1; myb88* (n=589) embryo sacs had four discernible cells. Strikingly, 44% and 22% of the mutant ovules appeared to contain cellular structures harbouring one or more prominent large cells and did not resemble mature female gametophytes (Fig. 3B, 3D). Another difference between the abnormal *flp-7* and *flp-1; my88* ovules and wild-type ovules was also observed. In the wild type, the growth and expansion of the embryo sac is accompanied by the degeneration of cells in the proximal nucellar region. However, in the abnormal *flp* ovules, these proximal cells persist (Fig. 3B, 3D).

In order to identify and compare the cell types present in embryo sacs at FG7 in wild-type and mutant ovules, specific markers were crossed into the *flp-7* mutant background. *ET884* has been shown to drive expression in both synergids at the micropylar end of the wild-type embryo sac (Gross-Hardt *et al*., 2007). However, the expression of this marker was observed in fewer *flp-7* ovules compared with the wild type (Fig. 4C). In the wild type, 76% of the observed ovules (n=361) had *ET884* expression, while in *flp-7* only 14% of the observed ovules (n=356) expressed the synergid maker. No expression of *ET884* was observed in those *flp-7* ovules in which no embryo sac could be distinguished (Fig. 4B). The egg cell-specific marker *ET1119* (Gross-Hardt *et al*., 2007) was also examined. Relatively few *flp-7* ovules sampled expressed this marker (3%, n=430) (Fig. 4F). In contrast, 48% of wild-type ovules sampled (n=250) displayed *ET1119* expression while the remainder did not. *ET1119* expression was never seen in ovules with abnormal embryo sac development (Fig. 4E). Finally, expression of two markers of central cells, *pMEA::GUS* (Gross-Hardt *et al*., 2007) and *AGL61::GFP* (Steffen *et al*., 2008), was analysed in wild-type and *flp-7* ovules. Consistent with the above results, the expression of the central cell markers was less frequent in *flp-7* than in wild-type ovules (Fig. 4I; Supplementary Fig. S3 at *JXB* online). *pMEA::GUS* expression in the wild type was found in 49% of ovules (n=279) but only in 12% (n=243) of *flp-7* ovules. No *pMEA::GUS* expression was seen in ovules containing abnormal embryo sacs (Fig. 4H). Results with *AGL61::GFP* were similar (Supplementary Fig. S3). Taken together, these data suggest that the aborted *flp-7* ovules lack differentiated female gametophytes and thus are incapable of being fertilized.

Comparison of structural development of the female gametophyte in the flp-7 *mutant and wild type*

To investigate the basis of the *flp-7* phenotype and the origin of the large cells seen in FG7 ovules of the mutant, a stage wise comparison of development was carried out by examining cleared ovules using DIC microscopy. Stages of ovule and female gametophyte development are summarized in Supplementary Table S4 at *JXB* online, based on Smyth *et al*. (1990) and Schneitz *et al*. (1995). Early stages were normal in *flp-7*, such as the appropriate initiation of ovule primordia (data not shown). In addition, both wild-type and *flp-7* pre-meiotic ovules (stage 2-III of ovule development; see Supplementary Table S4) displayed clearly differentiated MMCs (Fig. 5A, 5D). In L. *er* wild type stage 2-V, after meiosis, a clear tetrad of megaspores can be seen (Fig. 5B, Table 3). However, many of the

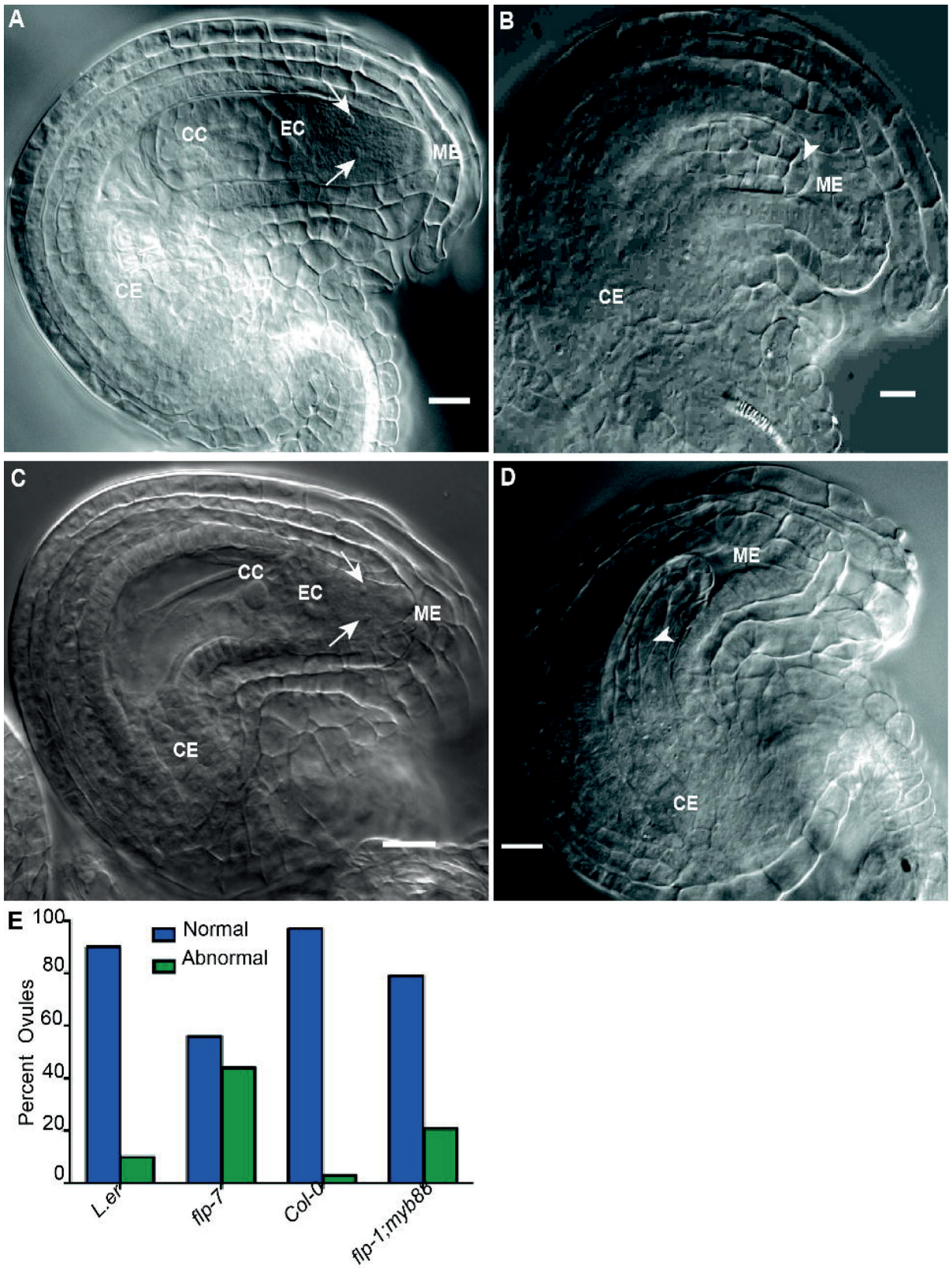

Fig. 3. Loss of *FLP* and/or *MYB88* leads to abnormal nucellar structures. (A–D) DIC micrographs of FG7 ovules containing mature female gametophytes. (A) Col-0. (B) *flp-1; myb88*. (C) L. *er*. (D) *flp-7*. (E) Quantification of embryo sac defects. CC, central cell; CE, chalazal end of the embryo sac; EC, egg cell; ME, micropylar end of the embryo sac. Arrows indicate synergid cells, and arrowheads indicate large cells found in abnormal *flp* ovules in the region where an embryo sac would normally form.

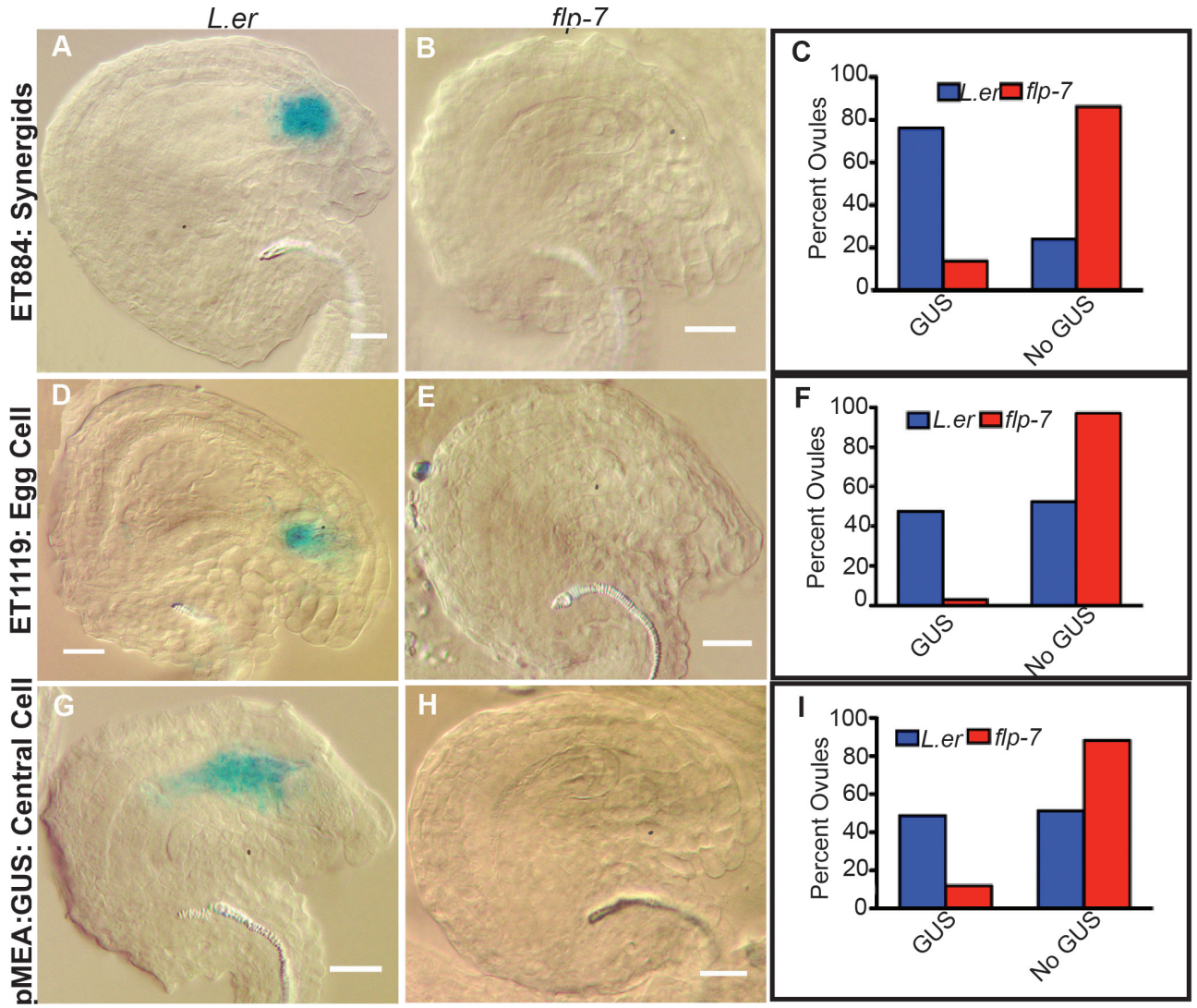

Fig. 4. *flp-7* morphologically abnormal ovules do not contain differentiated female gametophytes. (A, B, D, E, G, H) Micrographs of GUS-stained ovules. (A) In L. *er* embryo sacs, *ET884* is expressed in the synergids. (B) Abnormal *flp-7* ovules do not express this marker. (C) Quantification of expression. (D) In L. *er* embryo sacs, *ET1119* expression is found in the egg cell. (E) Abnormal *flp-7* ovules do not express this marker. (F) Quantification of expression. (G) In L. *er* embryo sacs, *pMEA:GUS* is expressed in the central cell. (H) Abnormal *flp-7* ovules do not express this marker. (I) Quantification of expression.

flp-7 ovules at comparable stages contain an abnormal number of cells in the region where the megaspores should be, including one large cell (Fig. 5E, Table 3). Normally during stage 3-I, the three non-functional megaspores begin to degenerate, leaving a mononuclear embryo sac (Fig. 5C). However, in similarly staged *flp-7* ovules, no cellular degeneration was found (Fig. 5F, Table 3). At stage 3-II, the embryo sac normally undergoes its first mitotic division producing a cell with two nuclei (Fig. 5G). Abnormal *flp-7* ovules display no such nuclear division and contain a single larger MMC- or megaspore-like cell as well as no (Fig. 5M), two (Fig. 5J), or three (Fig. 5N) other cells nearby. By stage 3-IV, the wild-type female gametophyte contains four nuclei (Fig. 5H), but these were not present in *flp-7* ovules (Fig. 5K). At stage 3-VI the embryo sac begins differentiation and cellularization in L. *er* (Fig. 5I). However, in abnormal *flp-7* ovules, instead of an embryo sac forming, a single large cell can be seen and is associated with a variable number of other cells (Fig. 5L, 5O). These results suggest that the MMC meiosis either did not occur or was abnormal.

The lowered expressivity of embryo sac defects in *flp-1; myb88* mutants made a detailed developmental study of embryo sac defects difficult. However, examination of mature embryo sacs of this genotype reveals that many (22%) contained abnormal structures that do resemble embryo sacs but rather contain a large cell resembling the MMC in position and size (Fig. 3D). This suggests that, similar to *flp-7*, *flp-1; myb88* MMCs undergo abnormal meiosis.

The expressivity of female gametophytic defects caused by loss of FLP *and/or* MYB88 *is influenced by genetic background*

Although a number of *flp* alleles and allelic combinations with *myb88* show significant reductions in fertility from their wild

types, there is variability in the expressivity of the phenotype, with seed set varying from 6% to 72% (Table 1), although the penetrance is complete (data not shown). Examination of the pattern of severity reveals that *flp* alleles in the L. *er* ecotype background exhibit more phenotypic severity than those in Col-0 (Table 1). In addition, crossing *flp-7* into the Col-0 background reduces the severity of the fertility defect (Table 1), supporting the hypothesis that either the L. *er* background harbours enhancers of the *flp* phenotype or Col-0 has suppressors of the *flp* phenotype, or both.

Many genetic differences exist between L. *er* and Col-0, including both single nucleotide polymorphisms and larger scale indels (Schmid *et al*., 2003; Ziolkowski *et al*., 2009). A prominent difference is the presence of a mutated *ERECTA* (*ER*) locus in L. *er*. *ER* and its family members, *ERECTA LIKE1* (*ERL1*) and *ERECTA LIKE2* (*ERL2*), encode leucine-rich repeat (LRR) domain-containing receptor-like kinases. They function in the stomatal patterning along with the TOO MANY MOUTHS (TMM) LRR receptor-like protein (Nadeau and Sack, 2002; Shpak *et al*., 2005). ER and its family members act upstream of FLP and MYB88. *ER* is the most important gene in its family and masks the functions of its paralogues. The *ER* family members also function in female reproductive development (Pillitteri *et al*., 2007). In *er-105; erl1-2; erl2-1*/+ ovules, cell proliferation in integuments is reduced, gametophytes abort, and cyclin A-encoding genes are misregulated. It

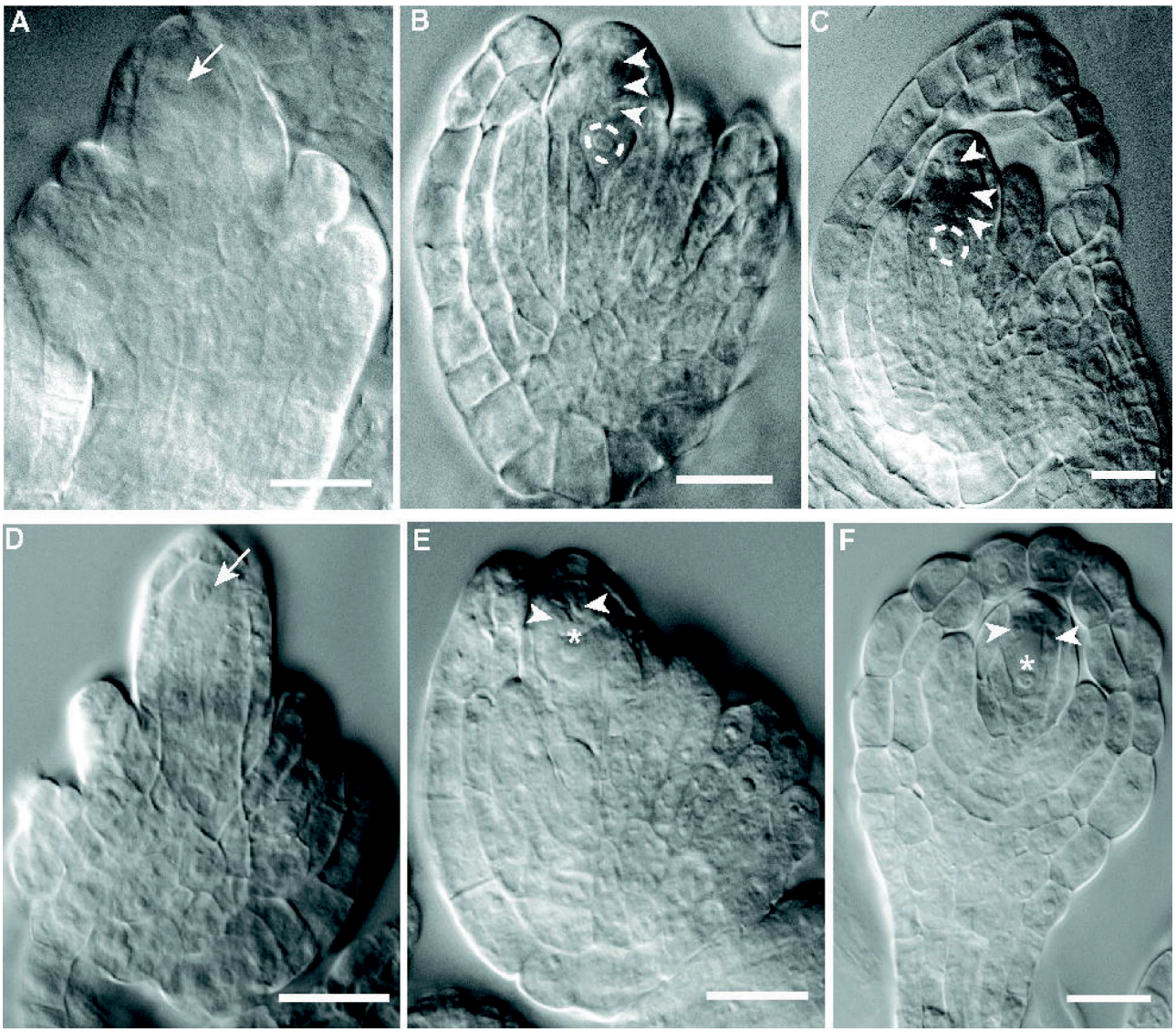

Fig. 5. Stages of female gametophyte development in the wild type and *flp-7* mutant. Ovule stages were determined from the development of the sporophyte using the nomenclature of Schneitz *et al.* (1995); see Supplementary Table S4 at *JXB* online. (A–O) DIC micrographs of ovules at different stages. (A, B, C, G, H, I) L. *er*. (D, E, F, J, K, L, M, N, O) *flp-7*. (A, D) Stage 2-III (pre-meiotic) with large MMCs near the tip of the nucellus (arrows). (B) Stage 2-V with tetrad of four megaspores (primary megaspore indicated by a dashed circle) in L. *er*. (C) At stage 3-I, the three non-functional megaspores begin to degenerate in L. *er*. (E) Varying numbers of cells are seen in *flp-7* ovules. Here, three cells can be seen (two toward the apex, arrowheads; and a larger cell more basally, asterisk). (F) The abnormal cells formed in *flp-7* ovules do not appear to be degenerating.

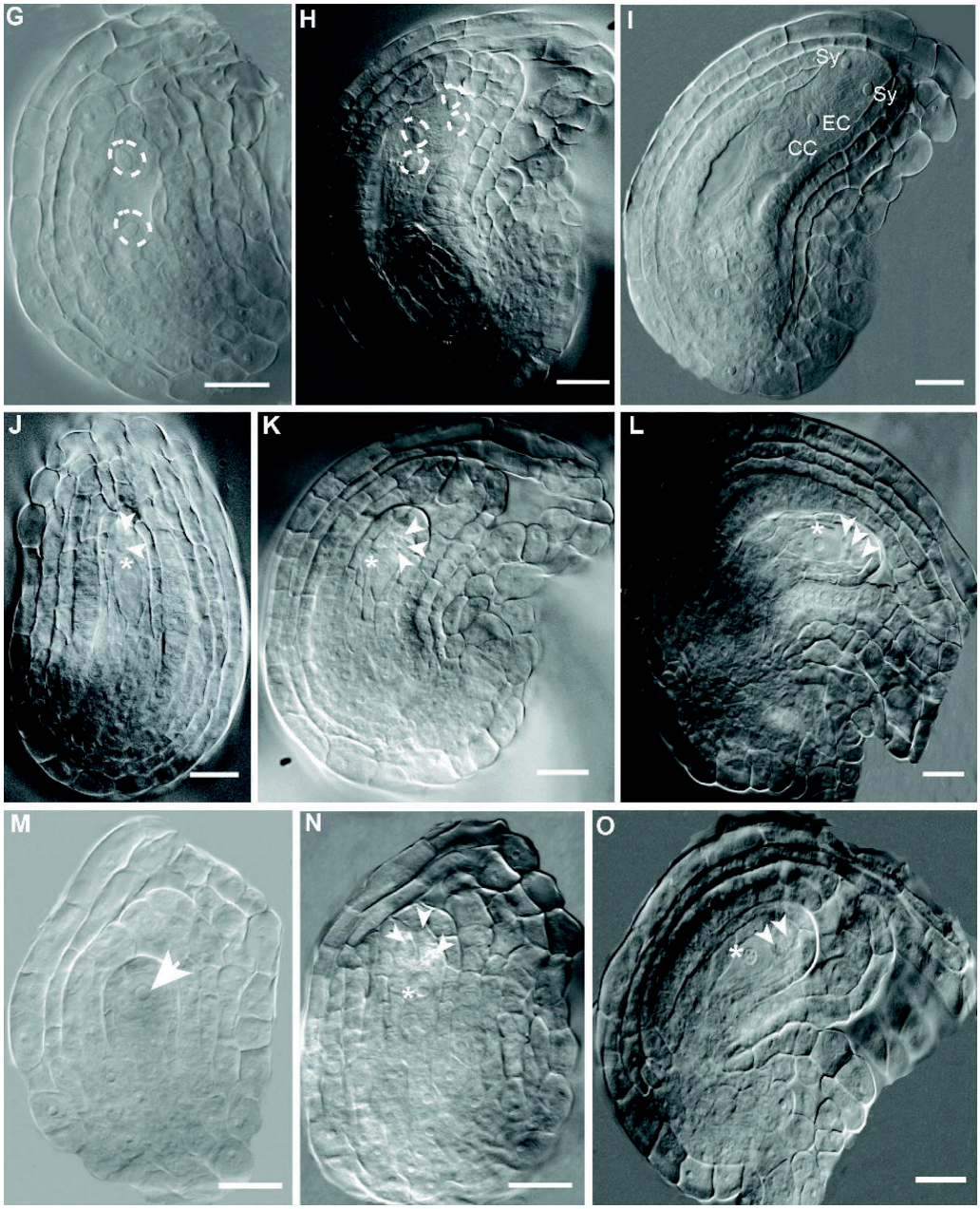

Fig. 5. *Continued*
(G) At stage 3-II, the first mitotic division of the megaspore to give rise to a two-nuclei (circled by dashed lines) female gametophyte in L. *er*. (J, M, N) No corresponding nuclear division can be seen in abnormal stage 3-II *flp-7*ovules; instead, a large cell remains with either zero (M), two (J), or three (N) other cells attached. (H) At stage 3-IV, a female gametophyte with four nuclei (dashed circles) is seen in L. *er*. In addition, the other cells of the nucellus have begun degenerating. (K) No such structures were seen in *flp-7* ovules; instead the abnormal cells remain. (I) By stage 3-VI, the embryo sac has begun differentiating and cellularizing in L. *er*. (L, O) In *flp-7* a single large cell is associated with a variable number of other cells (three in L, two in O). Asterisks indicate MMC-like/functional megaspore-like cells seen in *flp-7* ovules. Arrowheads indicate megaspores in L. *er* and cells associated with the MMC-like/functional megaspore-like cell in *flp-7*

was hypothesized that the mutant *er* locus in L. *er* influences the expressivity of *flp* alleles and may sensitize the ovule to loss of *FLP* function. To test these hypotheses, the *er* allele was complemented in the *flp-7* mutant background by transforming L. *er* and *flp-7* plants with an *ER* genomic rescue construct (a kind gift of Dr Keiko Torii). Complementing the defect in *er* in the *flp-7* background increased the seed set from 6% to 31% (Table 1), suggesting that this mutation accounts for some of the increased expressivity of female gametophyte defects in *flp-7* compared with *flp-1; myb88*. Restoration of wild-type ER activity also reduced the number of ovules per silique (Table 1) and reduced the severity of the stomatal defect (data not

Table 3. Phenotypic analysis of MMC division products during ovule development in the wild type and mutants

Ovule stage[a]	Genotype	One cell[b]	Two cells	Four cells	>4 cells	Total ovules observed
3-I	L. *er*	57% (99)	31% (54)	10% (17)	2% (3)	173
	flp-7	68% (186)	15% (40)	17% (47)	NO[c]	273
3-II	L. *er*	3% (5)	49% (77)	40% (63)	8% (13)	158
	flp-7	39% (18)	41% (19)	13% (6)	7% (3)	46
3-IV	L. *er*	6% (3)	NO	55% (27)	39% (19)	49
	flp-7	54% (41)	NO	21% (16)	25% (19)	76
3-VI	L. *er*	6% (12)	1% (2)	67% (137)	26% (54)	205
	flp-7	58% (82)	NO	28% (40)	13% (19)	141

[a] Stages according to Schneitz *et al.* (1995).
[b] The number in parentheses indicates the number of ovules observed.
[c] NO, none observed.

shown). However, *ER* complementation did not restore fertility to wild-type levels, suggesting that other genetic differences account for the remaining difference in expressivity between L. *er* and Col-0.

Discussion

In all sexually reproducing organisms, haploid gametes are formed after meiosis, either directly as in animals or indirectly after mitotic divisions as in plants. Therefore, meiosis is the key step leading to gametogenesis (van Werven and Amon, 2011). In angiosperms, although there is sexual dimorphism between the MMC and the male microspore mother cell, most mutations affecting meiosis affect both sexes. However, not all genes implicated in meiosis affect both male and female reproductive development (Ma, 2006). Broadly speaking, genes that have roles in megasporogenesis and megagametogenesis can be divided into sporophytic-acting and gametophytic-acting groups. Sporophytically acting genes with specific roles in regulating gametogenesis exhibit defects in spore and/or gamete formation but not in sporophytic parts of the ovule (Schneitz *et al*., 1997).

In this work, it was shown that a variety of loss-of-function, although not RNA null, *flp* alleles alone and in combination with *myb88* exhibit reduced seed set due to reduced female fertility (Fig. 2, Tables 1, 2). A defect in female but not male fertility is consistent with the low expression of *FLP* and *MYB88* in stamens and pollen (Zimmermann *et al*., 2004, 2005; Lai *et al*., 2005; this study). The female infertility of *flp* and *flp; myb88* mutants is not due to major defects in overall ovule morphology (Fig. 3B, 3D). In addition, mucilage is produced normally by mutant seed coats (Supplementary Fig. S1 at *JXB* online), suggesting that seed coat differentiation is relatively normal. However, examination of mature ovules revealed that abnormal *flp-7* and *flp-1; myb88* ovules did not contain embryo sacs; rather, they contained cellular structures with a larger single cell located close to the micropylar end of the ovule (Fig. 3B, 3D). These structures do not contain differentiated synergids, egg cells, or central cells (Fig. 4; Supplementary Fig. S3). Examination of earlier stages in ovule development revealed that these abnormal ovules arise due to a partially expressed defect in entry into meiosis by the MMC and/or abnormal meiosis and lack of megaspore differentiation (Fig. 5). Several lines of evidence support this interpretation. First, mature mutant ovules harboured a single large cell that resembles an MMC or a megaspore in position and size and which was accompanied by variable numbers of cells that appeared to arise from the same division (Figs 3, 5). Secondly, the retention of proximal nucellar cells in abnormal *flp-7* and *flp-1; myb88* ovules suggests that embryo sacs are absent, consistent with phenotypes seen before in other embryo sac absent mutants, including those with defects in meiosis of the MMC (Siddiqi *et al*., 2000). Thirdly, the smaller of the presumed division products of the MMC seen in *flp* mutants are positioned nearer the antipodal end of the ovule, where the non-functional megaspores are positioned in the wild type, while the large cell is nearer to the chalazal end, where the functional megaspore operates (Figs 3, 5). However, these smaller cells do not degenerate as normally the smaller megaspores would. Similar observations have been reported in *Arabidopsis* mutants where meiosis is incomplete or otherwise abnormal (Chen *et al*., 2011). Taken together, these results suggest that the paralogous FLP and MYB88 transcription factors function in the ovule to control entry into and progression through megasporogenesis, although they do not appear to function in male reproductive development, consistent with expression analysis.

FLP and *MYB88* are required to limit cell divisions in the stomatal lineage; *flp* and *flp; myb88* double mutant GMCs undergo extra divisions, resulting in stomatal clusters (Yang and Sack, 1995; Lai *et al*., 2005; Xie *et al*., 2010a). They perform this function by regulating expression of cell cycle genes (Xie *et al*., 2010a; Vanneste *et al*., 2011). FLP directly represses expression of the *CDKB1;1* gene (encoding a cyclin-dependent kinase that promotes entry into mitosis) after the symmetric division of the GMC, thereby preventing further division and forming a functional two-celled stoma (Xie *et al*., 2010a). The A2-type cyclin CYCA2;3 can form a functional complex with CDKB1;1 (Boudolf *et al*., 2009) and its expression is also directly and coordinately repressed by FLP/MYB88 in young guard cells (Vanneste *et al*., 2011). It has been demonstrated here that a larger number of ovules are formed in *flp* and *flp; myb88* mutants (Table 1). The molecular events that regulate development of the placenta, from which ovules are formed, is not well understood; however, an increase in the number of ovules suggests either

increased or extended proliferation to create a larger placenta or more entry into organogenesis by cells of this tissue. It is possible that the placental phenotype seen in *flp; myb88* mutants might also be due to lack of repression of similar cell cycle genes they repress during stomatal development. Alternatively, it has been shown that down-regulation of cytokinin signalling and metabolism takes place within the stomatal lineage and that this might be important for the transition from proliferation to differentiation (Pillitteri *et al*., 2011). Mutations in the *CKX3* and *CKX5* genes, which encode cytokinin oxidase/dehydrogenase enzymes functioning in degradation of this hormone, lead to increased proliferation in the placenta, supernumerary ovules, and increased seed set (Bartrina *et al*., 2011), suggesting that levels of cytokinin are important to regulate the size of this tissue. Therefore, FLP and MYB88 might also influence ovule number by regulating cytokinin signalling or homeostasis. Orthologues of *FLP* and *MYB88* in seed crop plants could be involved in control of ovule number (and therefore yield) and would be interesting targets for modification in such crops.

The role of cell cycle genes in controlling *Arabidopsis* meiosis is not well understood. In mammals, type A1 cyclins have been shown to function in the meiotic cell cycle (Wolgemuth, 2011). This appears be true for *Arabidopsis*. *CYCA1;2/TARDY ASYNCHRONOUS MEIOSIS* (*TAM*) is required for entry into both the first and second meiotic divisions (d'Erfurth *et al*., 2010). Such genes may be potential targets of FLP/MYB88. Suppression of mitotic genes such as *CDKB1;1* and/or *CYCA2;3* by FLP/MYB88 could also be necessary to allow entry into meiosis. This would be consistent with the necessity to suppress these genes for entry into the endocycle (Boudolf *et al*., 2009) and is also consistent with the finding that meiotic arrest can be caused by a failure to regulate CDK activity appropriately (Bulankova, 2010). It is reasonable to hypothesize that FLP and MYB88 function to regulate expression of cell cycle genes controlling meiotic entry and progression. During both stomatal development (Lai *et al*., 2005; Xie *et al*., 2010a) and placenta development (this study), FLP and MYB88 appear to inhibit expression of genes that positively regulate cell division. Based on the defects seen in meiosis in *flp* mutants (Fig. 5), they would appear to promote meiotic division, but might also do this by repression of mitotic promoting factors.

Loss of *FLP* or *FLP/MYB88* function does not lead to complete loss of female fertility. This incomplete expressivity could be due to a number of factors. The *FLP* alleles available are not RNA nulls (Lai *et al*., 2005). Therefore, it is possible that none of them is functionally null and there is residual *FLP* function present that is able to support meiosis in many ovules. Alternatively, other as yet unidentified genes could be partially functionally redundant with *FLP/MYB88*, allowing some female fertility in the *flp; myb88* mutants. However, it is clear that genetic background impacts the expressivity of the loss of *FLP* and/or *MYB88* function. Although all the *flp* alleles examined have reduced seed set, the *flp-7* allele in the L. *er* ecotype is the most severe, even more than the similar *flp-1* allele in Col-0 or *flp-7; myb88* in which *flp-7* has been introgressed into the Col-0 background (Table 1). Interestingly, the *flp-7* stomatal phenotype is also stronger than that of *flp-1* (Lai *et al*., 2005). Differences between genetic backgrounds in mutant penetrance, expressivity, and/or phenotype have been documented in *Arabidopsis* previously (e.g. Sedbrook *et al*., 2004; Sugliani *et al*., 2009). Many differences are present between L. *er* and Col-0 (Schmid *et al*., 2003; Ziolkowski *et al*., 2009), including in the *ER* gene. *ER* and its family members *ERL1* and *ERL2* have diverse roles coordinating cell proliferation with differentiation (Torii *et al*., 1996; Shpak *et al*., 2003, 2004, 2005; Pillitteri *et al*., 2007; Hord *et al*., 2008). ER family members act in complexes with TMM in GMCs (Lee *et al*., 2012) and act synergistically in enforcing stomatal patterning by interacting with the secreted peptides EPIDERMAL PATTERNING FACTORS (EPFs) (Hara *et al*., 2007, 2009; Hunt and Gray, 2009; Lee *et al*., 2012). These peptides function upstream of FLP/MYB88 in the stomatal lineage (Shpak *et al*., 2005). ER family members also ensure the proper growth of integuments and the progression of the mitotic cell cycle in the female gametophyte in a dosage-dependent manner (Pillitteri *et al*., 2007). The mutant *er* allele found in the L. *er* background might increase sensitivity to loss of *FLP* function. Indeed, when this mutation was complemented in the *flp-7* background, ovule number was reduced, seed set was improved (Table 1), and the stomatal defects were ameliorated (data not shown). The smaller number of ovules which form when *ER* function is restored is expected since *ER* also can control ovule number per fruit (Alonso-Blanco *et al*., 1999). The present results imply that ER also regulates entry of the MMC into meiosis. Complementation results support the hypothesis that loss of *ER* function provides a sensitized background for the loss of other genes, such as *FLP*, that function in common pathways. However, additional genetic changes must also contribute to the differential phenotypic expressivity, since *ER* complemented *flp-7* plants still display more severe phenotypes than similar mutations in the Col-0 background.

Supplementary data

Supplementary data are available at *JXB* online.

Supplementary Figure S1. Mucilage production is intact in *flp-7* and *flp-1; myb88* seeds.

Supplementary Figure S2. Pollen tube growth is not inhibited in *flp-7* pistils.

Supplementary Figure S3. Abnormal *flp-7* ovules do not express *AGL61:GFP*.

Supplementary Table S1. Primer combinations used for PCR genotyping.

Supplementary Table S2. Primers used in this study.

Supplementary Table S3. Female gametophyte markers used in this study.

Supplementary Table S4. Stages of floral, ovule, and gametophyte development.

Acknowledgements

The authors thank Dr Zidian Xie for advice and sharing of data before publication, Qin Lei for technical assistance, and two anonymous reviewers, members of the Lamb lab, and Dr Iris Meier (Ohio State University) for discussions. Dr Steffen Vanneste (Ghent University), Dr Ueli Grossniklaus (University of Zurich), and Dr Gary Drews (University of Utah) provided seeds, and

Dr Keiko Torii provided the *ERp::ER* plasmid used for complementation experiments. This work was supported in part by a grant from the National Science Foundation to RSL and funds from The Ohio State University.

References

Alonso-Blanco C, Blankestijn-de Vries H, Hanhart CJ, Koornneef M. 1999. Natural allelic variation at seed size loci in relation to other life history traits of Arabidopsis thaliana. *Proceedings of the National Academy of Sciences*, *USA* **96,** 4710–4717.

Alvarez J, Smyth DR. 1999. CRABS CLAW and SPATULA, two Arabidopsis genes that control carpel development in parallel with AGAMOUS. *Development* **126,** 2377–2386.

Bartrina I, Otto E, Strnad M, Werner T, Schmulling T. 2011. Cytokinin regulates the activity of reproductive meristems, flower organ size, ovule formation, and thus seed yield in Arabidopsis thaliana. *The Plant Cell* **23,** 69–80.

Berger F, Twell D. 2011. Germline specification and function in plants. *Annual Review of Plant Biology* **62,** 461–484.

Boudolf V, Barroco R, Engler Jde A, Verkest A, Beeckman T, Naudts M, Inze D, De Veylder L. 2004. B1-type cyclin-dependent kinases are essential for the formation of stomatal complexes in Arabidopsis thaliana. *The Plant Cell* **16,** 945–955.

Boudolf V, Lammens T, Boruc J, *et al.* 2009. CDKB1;1 forms a functional complex with CYCA2;3 to suppress endocycle onset. *Plant Physiology* **150,** 1482–1493.

Bulankova P R-KN, Nowack MK, Schnittger A, Riha K. 2010. Meiotic progression in Arabidopsis is governed by complex regulatory interactions between SMG7, TDM1, and the meiosis I-specific cyclin TAM. *The Plant Cell* **22,** 3791–3803.

Chen Z, Higgens JD, Hui JTL, Li J, Franklin FCH, Berger F. 2011. Retinoblastoma protein is essential for early meiotic events in Arabidopsis. *EMBO Journal* **30,** 744–755.

Christensen CA, King EJ, Jordan JR, Drews GN. 1997. Megagametogenesis in Arabidopsis wild type and the Gf mutant. *Sexual Plant Reproduction* **10,** 49–64.

Colombo M, Masiero S, Vanzulli S, Lardelli P, Kater MM, Colombo L. 2008. AGL23, a type I MADS-box gene that controls female gametophyte and embryo development in Arabidopsis. *The Plant Journal* **54,** 1037–1048.

Debeaujon I, Leon-Kloosterziel KM, Koornneef M. 2000. Influence of the testa on seed dormancy, germination and longevity in Arabidopsis. *Plant Physiology* **22,** 403–413.

d'Erfurth I, Cromer L, Jolivet S, Girard C, Horlow C, Sun Y, To JP, Berchowitz LE, Copenhaver GP, Mercier R. 2010. The cyclin-A CYCA1;2/TAM is required for the meiosis I to meiosis II transition and cooperates with OSD1 for the prophase to first meiotic division transition. *PLoS Genetics* **6**, e1000989.

Gremski K, Ditta G, Yanofsky MF. 2007. The HECATE genes regulate female reproductive tract development in Arabidopsis thaliana. *Development* **134,** 3593–3601.

Gross-Hardt R, Kagi C, Baumann N, Moore JM, Baskar R, Gagliano WB, Jurgens G, Grossniklaus U. 2007. LACHESIS restricts gametic cell fate in the female gametophyte of Arabidopsis. *PLoS Biology* **5**, e47.

Hara K, Kajita R, Torii KU, Bergmann DC, Kakimoto T. 2007. The secretory peptide gene EPF1 enforces the stomatal one-cell-spacing rule. *Genes and Development* **21,** 1720–1725.

Hara K, Yokoo T, Kajita R, Onishi T, Yahata S, Peterson KM, Torii KU, Kakimoto T. 2009. Epidermal cell density is autoregulated via a secretory peptide, EPIDERMAL PATTERNING FACTOR 2 in Arabidopsis leaves. *Plant and Cell Physiology* **50,** 1019–1031.

Heisler MG, Atkinson A, Bylstra YH, Walsh R, Smyth DR. 2001. SPATULA, a gene that controls development of carpel margin tissues in Arabidopsis, encodes a bHLH protein. *Development* **128,** 1089–1098.

Hord CL, Sun YJ, Pillitteri LJ, Torii KU, Wang H, Zhang S, Ma H. 2008. Regulation of Arabidopsis early anther development by the mitogen-activated protein kinases, MPK3 and MPK6, and the ERECTA and related receptor-like kinases. *Molecular Plant* **1,** 645–658.

Hunt L, Gray JE. 2009. The signaling peptide EPF2 controls asymmetric cell divisions during stomatal development. *Current Biology* **19,** 864–869.

Jefferson RA, Kavanagh TA, Bevan MW. 1987. GUS fusions: β-glucuronidase as a sensitive and versatile gene fusion marker. *EMBO Journal* **6,** 3901–3907.

Jiang L, Yang SL, Xie LF, Puah CS, Zhang XQ, Yang WC, Sundaresan V, Ye D. 2005. VANGUARD1 encodes a pectin methylesterase that enhances pollen tube growth in the Arabidopsis style and transmitting tract. *The Plant Cell* **17,** 584–596.

Lai LB, Nadeau JA, Lucas J, Lee EK, Nakagawa T, Zhao L, Geisler M, Sack FD. 2005. The Arabidopsis R2R3 MYB proteins FOUR LIPS and MYB88 restrict divisions late in the stomatal cell lineage. *The Plant Cell* **17,** 2754–2767.

Lee JS, Kuroha T, Hnilova M, Khatayevich D, Kanaoka MM, McAbee JM, Sarikaya M, Tamerler C, Torii KU. 2012. Direct interaction of ligand–receptor pairs specifying stomatal patterning. *Genes and Development* **26,** 126–136.

Ma H. 2006. A molecular portrait of Arabidopsis meiosis. *Arabidopsis Book* **4**, e0095.

Moore JM, Calzada JP, Gagliano W, Grossniklaus U. 1997. Genetic characterization of hadad, a mutant disrupting female gametogenesis in Arabidopsis thaliana. *Cold Spring Harbor Symposia on Quantitative Biology* **62,** 35–47.

Nadeau JA, Sack FD. 2002. Control of stomatal distribution on the Arabidopsis leaf surface. *Science* **296,** 1697–1700.

Neff MM, Neff JD, Chory J, Pepper AE. 1998. dCAPS, a simple technique for the genetic analysis of single nucleotide polymorphisms: experimental applications in Arabidopsis thaliana genetics. *The Plant Journal* **14,** 387–392.

Neff MM, Turk E, Kalishman M. 2002. Web-based primer design for single nucleotide polymorphism analysis. *Trends in Genetics* **18,** 613–615.

Pillitteri LJ, Bemis SM, Shpak ED, Torii KU. 2007. Haploinsufficiency after successive loss of signaling reveals a role for ERECTA-family genes in Arabidopsis ovule development. *Development* **134,** 3099–3109.

Pillitteri LJ, Peterson KM, Horst RJ, Torii KU. 2011. Molecular profiling of stomatal meristemoids reveals new component of asymmetric cell division and commonalities among stem cell populations in Arabidopsis. *The Plant Cell* **23,** 3260–3275.

Punwani JA, Rabiger DS, Drews GN. 2007. MYB98 positively regulates a battery of synergid-expressed genes encoding filiform apparatus localized proteins. *The Plant Cell* **19,** 2557–2568.

Rodrigo-Peiris T, Xu XM, Zhao Q, Wang HJ, Meier I. 2011. RanGAP is required for post-meiotic mitosis in female gametophyte development in Arabidopsis thaliana. *Journal of Experimental Botany* **62,** 2705–2714.

Schmid KJ, Sorensen TR, Stracke R, Torjek O, Altmann T, Mitchell-Olds T, Weisshaar B. 2003. Large-scale identification and analysis of genome-wide single-nucleotide polymorphisms for mapping in Arabidopsis thaliana. *Genome Research* **13,** 1250–1257.

Schneitz K, Hulskamp M, Kopczak SD, Pruitt RE. 1997. Dissection of sexual organ ontogenesis: a genetic analysis of ovule development in *Arabidopsis thaliana. Development* **124,** 1367–1376.

Schneitz K, Hulskamp M, Pruitt RE. 1995. Wild type ovule development in Arabidopsis thailana: a light microscope study of cleared whole mount tissue. *The Plant Journal* **7,** 731–749.

Sedbrook JC, Ehrhardt DW, Fisher SE, Scheible WR, Somerville CR. 2004. The Arabidopsis sku6/spiral1 gene encodes a plus end-localized microtubule-interacting protein involved in directional cell expansion. *The Plant Cell* **16,** 1506–1520.

Shpak ED, Berthiaume CT, Hill EJ, Torii KU. 2004. Synergistic interaction of three ERECTA-family receptor-like kinases controls Arabidopsis organ growth and flower development by promoting cell proliferation. *Development* **131,** 1491–1501.

Shpak ED, Lakeman MB, Torii KU. 2003. Dominant-negative receptor uncovers redundancy in the Arabidopsis ERECTA leucine-rich repeat receptor-like kinase signaling pathway that regulates organ shape. *The Plant Cell* **15,** 1095–1110.

Shpak ED, McAbee JM, Pillitteri LJ, Torii KU. 2005. Stomatal patterning and differentiation by synergistic interactions of receptor kinases. *Science* **309,** 290–293.

Siddiqi I, Ganesh G, Grossniklaus U, Subbiah V. 2000. The dyad gene is required for progression through female meiosis in Arabidopsis. *Development* **127,** 197–207.

Smyth DR, Bowman JL, Meyerowitz EM. 1990. Early flower development in *Arabidopsis. The Plant Cell* **2,** 755–767.

Springer PS, Holding DR, Groover A, Yordan C, Martienssen RA. 2000. The essential Mcm7 protein PROLIFERA is localized to the nucleus of dividing cells during the G(1) phase and is required maternally for early Arabidopsis development. *Development* **127,** 1815–1822.

Steffen JG, Kang IH, Portereiko MF, Lloyd A, Drews GN. 2008. AGL61 interacts with AGL80 and is required for central cell development in Arabidopsis. *Plant Physiology* **148,** 259–268.

Sugliani M, Rajjou L, Clerkx EJ, Koornneef M, Soppe WJ. 2009. Natural modifiers of seed longevity in the Arabidopsis mutants abscisic acid insensitive3-5 (abi3-5) and leafy cotyledon1-3 (lec1-3). *New Phytologist* **184,** 898–908.

Teotia S, Lamb RS. 2009. The paralogous genes RADICAL-INDUCED CELL DEATH1 and SIMILAR TO RCD ONE1 have partially redundant functions during Arabidopsis development. *Plant Physiology* **151,** 180–198.

Torii KU, Mitsukawa N, Oosumi T, Matsuura Y, Yokoyama R, Whittier RF, Komeda Y. 1996. The Arabidopsis ERECTA gene encodes a putative receptor protein kinase with extra cellular leucine-rich repeats. *The Plant Cell* **8,** 735–746.

Tran LS, Nakashima K, Sakuma Y, Simpson SD, Fujita Y, Maruyama K, Fujita M, Seki M, Shinozaki K, Yamaguchi-Shinozaki K. 2004. Isolation and functional analysis of Arabidopsis stress-inducible NAC transcription factors that bind to a drought-responsive cis-element in the early responsive to dehydration stress 1 promoter. *The Plant Cell* **16,** 2481–2498.

Unte US, Sorensen AM, Pesaresi P, Gandikota M, Leister D, Saedler H, Huijser P. 2003. SPL8, an SBP-box gene that affects pollen sac development in Arabidopsis. *The Plant Cell* **15,** 1009–1019.

Vanneste S, Coppens F, Lee E, *et al.*. 2011. Developmental regulation of CYCA2s contributes to tissue-specific proliferation in Arabidopsis. *EMBO Journal* **30,** 3430–3441.

van Werven FJ, Amon A. 2011. Regulation of entry into gametogenesis. *Philosophical Transactions of the Royal Society B: Biological Sciences* **366,** 3521–3531.

Wolgemuth DJ. 2011. Function of the A-type cyclins during gametogenesis and early embryogenesis. *Results and Problems in Cell Differentiation* **53,** 391–413.

Xie Z, Lee E, Lucas JR, Morohashi K, Li D, Murray JA, Sack FD, Grotewold E. 2010a. Regulation of cell proliferation in the stomatal lineage by the Arabidopsis MYB FOUR LIPS via direct targeting of core cell cycle genes. *The Plant Cell* **22,** 2306–2321.

Xie Z, Li D, Wang L, Sack FD, Grotewold E. 2010b. Role of the stomatal development regulators FLP/MYB88 in abiotic stress responses. *The Plant Journal* **64,** 731–739.

Yadegari R, Drews GN. 2004. Female gametophyte development. *The Plant Cell* **16** Suppl, S133–S141.

Yang M, Sack FD. 1995. The too many mouths and four lips mutations affect stomatal production in Arabidopsis. *The Plant Cell* **7,** 2227–2239.

Zimmermann P, Hennig L, Gruissem W. 2005. Gene-expression analysis and network discovery using Genevestigator. *Trends in Plant Science* **10,** 407–409.

Zimmermann P, Hirsch-Hoffmann M, Hennig L, Gruissem W. 2004. GENEVESTIGATOR. Arabidopsis microarray database and analysis toolbox. *Plant Physiology* **136,** 2621–2632.

Ziolkowski PA, Koczyk G, Galganski L, Sadowski J. 2009. Genome sequence comparison of Col and Ler lines reveals the dynamic nature of Arabidopsis chromosomes. *Nucleic Acids Research* **37,** 3189–3201.